



## Fabrication of high performance Pt counter electrodes on conductive plastic substrate for flexible dye-sensitized solar cells

Lili Chen<sup>a</sup>, Weiwei Tan<sup>b</sup>, Jingbo Zhang<sup>b</sup>, Xiaowen Zhou<sup>b</sup>, Xiaoling Zhang<sup>a,\*</sup>, Yuan Lin<sup>b,\*\*</sup>

<sup>a</sup> Department of Chemistry, School of Science, Beijing Institute of Technology, Beijing 100081, China

<sup>b</sup> Beijing National Laboratory for Molecular Sciences, Key Laboratory of Photochemistry, Institute of Chemistry, Chinese Academy of Sciences, ZhongGuanCun No. 2, 1st North Street, Beijing 100190, China

### ARTICLE INFO

#### Article history:

Received 20 November 2009

Received in revised form 25 January 2010

Accepted 30 January 2010

Available online 6 February 2010

#### Keywords:

Flexible Pt counter electrode

Chemical reduction

Hydrothermal treatment

Screen printing

Dye-sensitized solar cells

### ABSTRACT

Pt counter electrodes (CEs) with different platinum loading have been prepared using chemical reduced method on flexible indium-doped tin oxide coated polyethylene naphthalate (ITO-PEN) for dye-sensitized solar cells (DSSCs).  $\text{H}_2\text{PtCl}_6 \cdot 6\text{H}_2\text{O}$  terpineol solutions were screen printed on the transparent ITO-PEN substrates. After drying,  $\text{H}_2\text{PtCl}_6$  was reduced by treating it in  $\text{NaBH}_4$  solution followed by the hydrothermal treatment at  $100^\circ\text{C}$ . The obtained Pt CEs with different Pt-loading ( $2.4\text{--}7.7 \mu\text{g}/\text{cm}^2$ ) were characterized by SEM, XPS, electrochemical impedance and transmission spectrum measurement. The Pt CEs show high catalytic activity, low charge transfer resistance ( $0.26\text{--}1.38 \Omega \text{cm}^2$ ) and good light transmittance (about 70% at  $400\text{--}800 \text{ nm}$ ). The light-to-electricity conversion efficiency of the flexible DSSC fabricated with the prepared Pt CE and the  $\text{TiO}_2$  photoanode prepared on Ti substrate by screen printing technique attains 5.41% under the simulated AM 1.5 sunlight, which is almost same as that based on the thermal decomposed Pt CE on FTO-glass. Compared with other methods to prepare Pt CEs, chemical reduced method is simple and suitable for flexible polymer substrates and the large scale preparation of DSSCs.

© 2010 Elsevier Ltd. All rights reserved.

### 1. Introduction

Since O'Regan and Grätzel firstly reported dye-sensitized solar cell (DSSC) in 1991, it has attracted great interests in academic research and industrial applications due to its high light-to-electricity conversion efficiency, simple fabrication process and the potential for low cost production [1–3]. DSSC typically consists of redox electrolyte sandwiched by a nanocrystalline- $\text{TiO}_2$  film covered by a monolayer of dye molecules and a counter electrode (CE) with transparent conducting oxide (TCO) glass as substrates. The CE is used to reduce the redox species, which act as a mediator in regenerating the sensitizer after electron injection in a liquid-state DSSC, or to collect holes from the hole transport material in a solid-state DSSC [4]. In order to reduce cost and accelerate the applications of DSSCs, it is necessary to develop DSSCs based on flexible substrates such as metal foils and plastic substrates. However, there are few detailed reports on the preparation of CEs on plastic substrates.

Up to now, several kinds of catalytic materials for CEs, such as platinum [5–11], carbon materials (graphite, activated carbon, carbon black, single-wall carbon nanotubes) [12–17],

poly(3,4-ethylenedioxythiophene) (PEDOT) [18–22], poly(3,3-diethyl-3,4-dihydro-2H-thieno-[3,4-b][1,4]dioxepine) (PProDOT-Et<sub>2</sub>) [23], polypyrrole [24] and polyaniline [25], have been introduced. However, the best candidate for the CE is Pt due to its highly catalytic effect toward triiodide reaction, superior chemical and electrochemical stabilities.

Thermal decomposition of  $\text{H}_2\text{PtCl}_6$  isopropanol solution is widely used to prepare high performance Pt CE, because it is stable and shows higher exchange current density for the  $\text{I}_3^-/\text{I}^-$  couple [4]. However, this process requires a heat treatment up to  $390^\circ\text{C}$  that most plastic substrates cannot bear. Pt CEs on flexible substrates are usually prepared by sputtering, electrochemical deposition and chemical reduction. Ikegami et al. deposited a Pt/Ti bilayer on ITO-PEN substrates using vacuum sputtering and assembled a full plastic DSSC and achieved the conversion efficiency of 4.31% [10]. Pt CEs deposited by sputtering can be well used for flexible DSSC. Furthermore, Fang et al.'s investigation showed that the catalytic effect of sputtered Pt layer is independent of Pt layer thickness when it is over 7 nm [26]. Therefore, the inner Pt layer in thick sputtered films, such as 100 nm Pt-mirror layer, has no contribution on triiodide reduction and is waste. Electrochemical deposition method attracted much attention because it is simple and feasible. Grätzel electrodeposited Pt catalyst on the ITO/PEN substrate to assemble a flexible DSSC and achieved the conversion efficiency of 7.2% [27]. Chemical reduction of  $\text{H}_2\text{PtCl}_6$  to prepare Pt CE on plastic substrate has been studied by Kang et al. [28] and Park et al.

\* Corresponding author.

\*\* Corresponding author. Tel.: +86 10 82615031; fax: +86 10 82617315.

E-mail addresses: [ZhangXL@bit.edu.cn](mailto:ZhangXL@bit.edu.cn) (X. Zhang), [linyuan@iccas.ac.cn](mailto:linyuan@iccas.ac.cn) (Y. Lin).

[29]. They spread  $\text{H}_2\text{PtCl}_6 \cdot 6\text{H}_2\text{O}$  2-propanol solution on conductive plastic substrates followed by reducing  $\text{Pt}^{4+}$  in  $\text{NaBH}_4$  solution. However, there is no detailed investigation on the chemical reduction of Pt CE as to optimize its performance.

Based on these reports, we attempted to fabricate Pt CEs on flexible ITO/PEN substrates by screen printing technology followed by chemical reduction method. The ITO/PEN substrate is introduced in DSSCs by many scientists, but it cannot endure high temperature (<150 °C). Here, we reported for the first time the common pressure hydrothermal method as a post-treatment to treat Pt CEs at low temperature via a hydrothermal reaction at the solid/liquid interface. The common pressure hydrothermal method is a simple low temperature preparation method, where the hydrothermal reaction can take place in a non-sealed system at 100 °C at common pressure. It is convenient and cheap and can be used on the flexible polymer substrates. The organic residues can be removed and Pt CEs become mechanically stable after the hydrothermal process. In addition, it is also beneficial to the preparation of large scale cells and mass production. The prepared flexible Pt CEs were used to fabricate DSSCs with nanocrystalline- $\text{TiO}_2$  photoelectrodes deposited on Ti foil substrates by screen printing and high temperature sintering and the cells show satisfied photovoltaic performance.

## 2. Experimental

### 2.1. Materials

All chemicals used were of analytical reagent grade without further purification.  $\text{H}_2\text{PtCl}_6 \cdot 6\text{H}_2\text{O}$  was purchased from Sinopharm Chemical Reagent Beijing Co., Ltd. and other reagents from Aldrich. ITO-PEN (15  $\Omega/\square$ , light transmittance: 80% at 550 nm, Peccell Technologies, Inc.) and fluorine-doped tin oxide transparent conductive glass (FTO, 20  $\Omega/\square$ , Hake New Energy Co. Ltd., Harbin) were ultrasonically cleaned sequentially in detergent solution, acetone and finally in distilled water. Ti foil (0.2 mm thickness, Baoji Mingkun Nonferrous Metals Co., Ltd.) was washed with mild detergent and rinsed in distilled water, then immersed in saturated oxalic acid solution for 10 min and rinsed in distilled water again.

### 2.2. Preparation of Pt CEs

$\text{H}_2\text{PtCl}_6 \cdot 6\text{H}_2\text{O}$  was dissolved in terpineol with concentration of 0.4 wt%, 0.6 wt%, 0.8 wt% and 1.0 wt% to prepare the paste. As a low temperature method, the pastes were screen printed on the ITO-PEN surface using a 200 mesh screen and then dried at 80 °C for 2 h to give  $\text{H}_2\text{PtCl}_6$ /ITO-PEN electrodes with the active area of 1 cm  $\times$  1 cm. Then the  $\text{H}_2\text{PtCl}_6$ /ITO-PEN electrodes were immersed in 10 mM  $\text{NaBH}_4$  aqueous solution at 40 °C to reduce Pt ions. After 2 h, the electrodes were taken out from the  $\text{NaBH}_4$  solution and rinsed with distilled water. Then, two different post-treatment methods were applied. One is the common pressure hydrothermal process to place the electrodes in a non-sealed container filled with water at 100 °C for 4 h to remove organic residues then to dry them at 80 °C for 2 h giving transparent Pt CEs (Pt/ITO-PEN). Another is to sinter the electrodes at 100 °C for 4 h in an oven instead of the hydrothermal treatment. The thermal decomposed Pt CE was also prepared at 390 °C on FTO-glass for comparison [30].

### 2.3. Characterization of Pt/ITO-PEN films

The surface morphology of the Pt electrodes was observed by a scanning electron microscope (SEM, Hitachi S-4300). The transmission spectrum measurement was taken on a Hitachi U-3010 spectrophotometer.

To study the formation of Pt on ITO-PEN surface, X-ray photoelectron spectroscopy was obtained using an Escalab 220i-XL

spectrometer with standard Al K $\alpha$  radiation. The spectra were taken at a working pressure of  $<3 \times 10^{-9}$  mbar. The binding energy was calibrated using the C 1s line (284.6 eV) from adventitious carbon. Wide-scan spectra were recorded in the range of 0–1200 eV.

To study the interfacial charge transfer resistances ( $R_{ct}$ ), electrochemical impedance spectra (EIS) were measured on a symmetric thin-layer cell composed of two identical Pt electrodes and a Surlyn film with the thickness of 40  $\mu\text{m}$  as the spacer. The active area of the electrode was 0.25 cm $^2$ . The inter-space between electrodes was filled with electrolyte, which was 0.5 mol L $^{-1}$  LiI, 0.05 mol L $^{-1}$  I $_2$ , and 0.5 mol L $^{-1}$  4-*tert*-butylpyridine in 3-methoxypropionitrile. The measurement was performed using Solartron 1255B frequency response analyzer and Solartron SI 1287 electrochemical interface system at the zero bias with the frequency range of 0.05 Hz to 1 MHz.

Platinum loadings were determined by dissolution of the electrode in nitrohydrochloric acid, and platinum content in the subsequent diluted solution was determined by measuring its atomic emission spectroscopy (Hitachi P-4010).

### 2.4. Fabrication of flexible DSSCs

A Ti foil was used as a substrate for the nanocrystalline- $\text{TiO}_2$  film to fabricate the flexible DSSC. The  $\text{TiO}_2$  colloidal was synthesized by sol-gel and hydrothermal techniques from titanium isopropoxide (97 wt%) precursor. The typical preparation process was as following. Titanium isopropoxide was hydrolyzed in pH 2 aqueous solution under strong stirring at 80 °C for 2 h and then autoclaved at 250 °C for 13 h [31]. The colloidal was evaporated and converted to a  $\text{TiO}_2$  screen printing paste [32], and then screen printed on the Ti foil surface using an 80 mesh screen. After drying at room temperature, the  $\text{TiO}_2$  thin films were sintered at 450 °C for 30 min in air to give nanocrystalline- $\text{TiO}_2$  films. As the  $\text{TiO}_2$  electrodes were cooled to 80 °C, they were sensitized by immersing in an absolute ethanolic solution of  $5 \times 10^{-4}$  mol L $^{-1}$  Ru(dcbpy) $_2$ (NCS) $_2$ (dcbpy: 2,2'-bipyridine-4,4'-dicarboxylic acid) (N $_3$ , Solaronix) for 12 h. The thickness of the nanocrystalline- $\text{TiO}_2$  film was fixed at about 10  $\mu\text{m}$  for flexible DSSC. The active cell area was 0.20 cm $^2$ . The electrolyte was 0.5 mol L $^{-1}$  LiI, 0.05 mol L $^{-1}$  I $_2$ , and 0.5 mol L $^{-1}$  4-*tert*-butylpyridine in 3-methoxypropionitrile.

Current–voltage (I–V) curves of DSSCs were measured with Potentiostat/Galvanostat Model 273 (EG&G) under light intensity of 100 mW cm $^{-2}$  at AM 1.5 offered by a solar light simulator (Oriol, 91160-1000).

## 3. Results and discussion

### 3.1. Preparation of flexible Pt CEs

The  $\text{H}_2\text{PtCl}_6$ /ITO-PEN electrodes prepared by screen printing the pastes on the ITO-PEN surface are transparent and colorless. When the  $\text{H}_2\text{PtCl}_6$ /ITO-PEN electrodes were immersed into the  $\text{NaBH}_4$  solution, the electrode surface starts to bubble up gently and color of the surface changes gradually from colorless to gray-white. At this point, the  $\text{Pt}^{4+}$  ions were reduced to metal platinum at the ITO-PEN surface according to the redox reactions,



The overall reaction,



To obtain the high performance flexible Pt CEs, we carefully optimized the concentration and pH of  $\text{NaBH}_4$  solution, the reaction temperature and time. These optimized reaction conditions were

stated in Section 2. In addition, the ITO/PEN substrate is so light that it can float on the solution surface, so the flexible electrodes were fixed on the container bottom by adhesive tape during the chemical reduced reaction and the hydrothermal treatment process.

### 3.2. Surface morphologies of Pt/ITO-PEN films

Fig. 1 shows the surface morphology of the bare ITO-PEN substrate and the Pt/ITO-PEN electrode prepared using 0.6 wt%  $\text{H}_2\text{PtCl}_6 \cdot 6\text{H}_2\text{O}$  terpineol solution. As seen in Fig. 1a, the surface of the bare ITO-PEN substrate is quite flat with a few particles with a size of  $\sim 100$  nm on the surface. Fig. 1b shows the surface morphology of Pt/ITO-PEN CE after the hydrothermal treatment. It can be found that small Pt nanoparticles formed the Pt nanoclusters with the size of  $\sim 10$  nm on the surface of ITO-PEN substrate. The surface morphology of the Pt/ITO-PEN electrodes based on other concentration of  $\text{H}_2\text{PtCl}_6 \cdot 6\text{H}_2\text{O}$  terpineol solutions is similar to that in Fig. 1b. Obviously, the ITO-PEN substrate was covered completely by Pt nanoparticles. In comparison, Fig. 1c shows the surface morphology of Pt/ITO-PEN CE directly dried at  $100^\circ\text{C}$  for 4 h in an oven instead of the hydrothermal treatment. On this Pt/ITO-PEN electrode surface, it was found the Pt nanoclusters are inhomogeneous and the shape of Pt nanoclusters is indistinct. In fact, after the  $\text{H}_2\text{PtCl}_6$ /ITO-PEN electrode was taken out from  $\text{NaBH}_4$  aqueous solution, there was some terpineol remaining on the surface. During the chemical reduced process, the terpineol plays a role as a protector to stabilize the Pt nanoclusters and prevent further growth of the Pt nanoparticles, which benefit to increase the surface area of Pt electrode. Then, in hydrothermal treatment process, the organic residues and the loose Pt nanoparticles were removed, as shown in Fig. 1b. In other words, the hydrothermal treatment, as a post-treatment, is more important and efficient than the drying method at  $100^\circ\text{C}$ .

### 3.3. Analysis of XPS spectrum of the Pt/ITO-PEN electrode

The formation of Pt on ITO-PEN surface after the hydrothermal treatment was determined using X-ray photoelectron spectroscopy (XPS). Fig. 2 shows a wide-scan spectrum for Pt film deposited on ITO-PEN surface (Fig. 2a) and the Pt 4f XPS peaks (Fig. 2b). There are no other Pt characteristic peaks except Pt 4f XPS peaks which appeared in Fig. 2a. In Fig. 2b, the XPS peaks with binding energies of  $\sim 71$  eV and  $\sim 74$  eV correspond to Pt  $4f_{7/2}$  and Pt  $4f_{5/2}$  [33], respectively. But the peak intensity ratio of Pt  $4f_{7/2}$  and Pt  $4f_{5/2}$  is not the same as the reported value of 7:5, indicating that there exist some other valence states of platinum on the ITO-PEN surface except Pt (0), but the main valence state of platinum was zero.

### 3.4. Transmission spectra and Pt-loading of Pt/ITO-PEN electrodes

Fig. 3 shows the transmission spectra of Pt/ITO-PEN CEs prepared with different concentrations of  $\text{H}_2\text{PtCl}_6$  solutions. The light transmittance for all Pt/ITO-PEN CEs is around 70%, and decreases with increasing the concentration of  $\text{H}_2\text{PtCl}_6$ . We can observe that the color of Pt/ITO-PEN CEs become darker and darker with increasing the  $\text{H}_2\text{PtCl}_6$  concentration. Due to the scatter effect of Pt nanoparticles on the ITO-PEN surface, the peaks in the transmission spectra move to long wavelength with the formation of larger Pt nanoparticles in the higher concentration of  $\text{H}_2\text{PtCl}_6$ . Considering illumination through the Pt CEs is required for DSSCs based on the photoelectrode on Ti foil substrates, the good light transmittance of the Pt/ITO-PEN CEs will be beneficial to high performance of the flexible DSSCs.

Inset of Fig. 3 shows the change of Pt-loading with the concentration of  $\text{H}_2\text{PtCl}_6$ . The Pt-loading increases with increase in the concentration of  $\text{H}_2\text{PtCl}_6$ . When the concentration of  $\text{H}_2\text{PtCl}_6$  is 0.4 wt%, 0.6 wt%, 0.8 wt% and 1.0 wt%, Pt-loading of the prepared electrodes is  $2.4 \mu\text{g}/\text{cm}^2$ ,  $3.5 \mu\text{g}/\text{cm}^2$ ,  $5.8 \mu\text{g}/\text{cm}^2$  and  $7.7 \mu\text{g}/\text{cm}^2$ ,

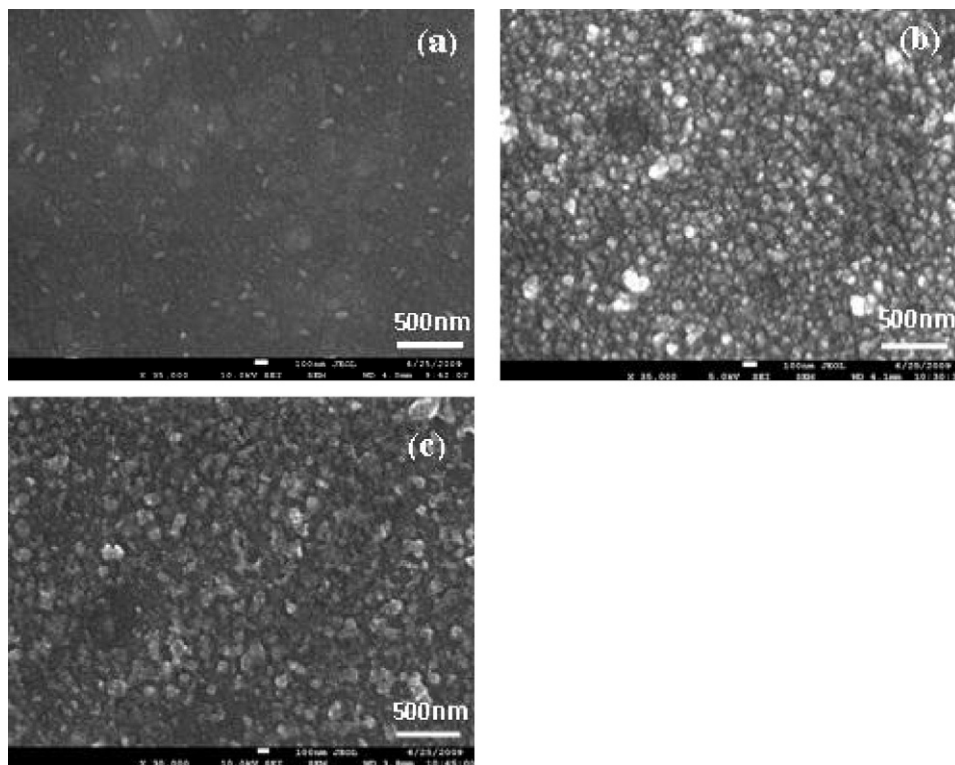


Fig. 1. Scanning electron microscopy images of bare ITO-PEN substrate (a), Pt electrodes prepared on ITO-PEN by chemical reduced deposition with hydrothermal treatment (b) and with drying at  $100^\circ\text{C}$  instead of hydrothermal treatment (c).

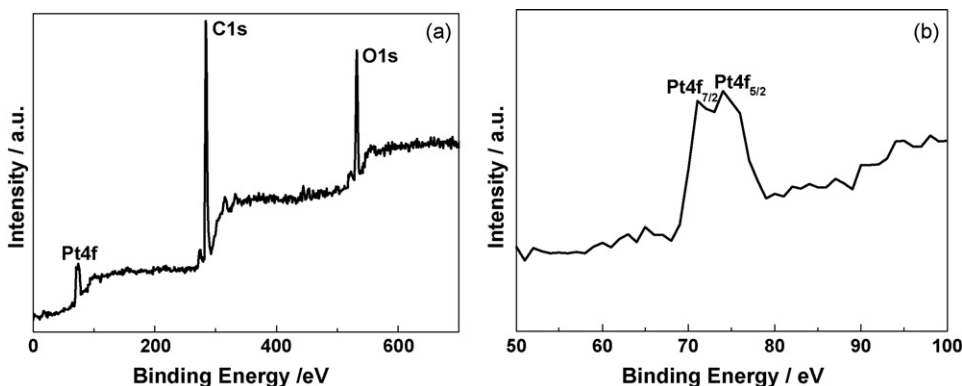


Fig. 2. Wide-scan XPS spectrum of Pt/ITO-PEN prepared by chemical reduced deposition with hydrothermal treatment (a) and its Pt 4f XPS spectrum (b).

respectively. The Pt-loading was controlled by the Pt precursor concentration, but it is not direct proportion.

### 3.5. Electrocatalytic activity of Pt/ITO-PEN electrodes

To understand electrocatalytic activity of the Pt CEs after the hydrothermal treatment, the electrochemical impedance spectroscopy (EIS) was measured with the sandwich type electrochemical cell consisting of two identical Pt/ITO-PEN electrodes shown in Fig. 4a [34]. For measurement convenience, the flexible cell was clamped between two pieces of glass as shown in Fig. 4a. The equivalent circuit for this type of cell is described in Fig. 4b. The ohmic serial resistance ( $R_s$ ) can be determined from the impedance at the high frequency (around 100 kHz) where the phase is zero. In the middle frequency range between 10 Hz and 100 kHz, the impedance was dominated by the RC network of Pt electrode and electrolyte interface, which consists of the charge transfer resistance ( $R_{ct}$ ) and capacitance of electrical double layer ( $C_{dl}$ ). The impedance in the low frequency can be interpreted to the Nernst diffusion impedance ( $Z_N$ ). The resultant impedance spectra are shown in Fig. 4c and the fitting data are listed in Table 1. The values of frequency at the highest points of the impedance spectra are indicated in the figure. The circle became small with increasing the concentration of  $H_2PtCl_6$  as shown in Fig. 4c, indicating the decrease of  $R_{ct}$ . Because Pt serves as a catalyst for triiodide reduction, the decrease in  $R_{ct}$  implies

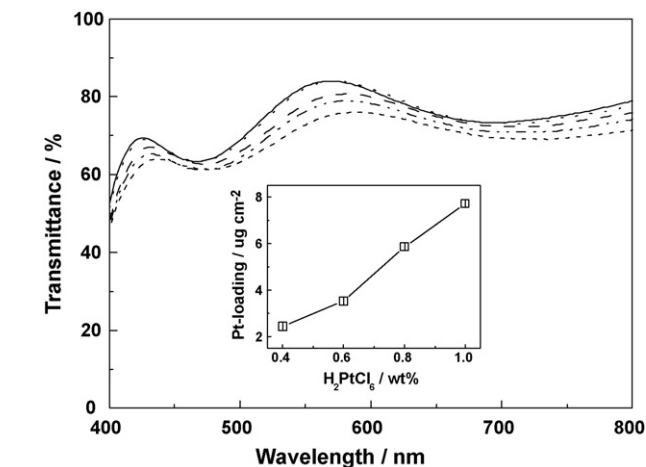


Fig. 3. Transmission spectra of ITO-PEN (solid line) and the flexible Pt counter electrodes prepared with the paste containing 0.4 wt% (dot line), 0.6 wt% (dash line), 0.8 wt% (dash dot dot line) and 1.0 wt% (short dash line)  $H_2PtCl_6 \cdot 6H_2O$  terpienol solutions. The inset shows the relationship of Pt-loading of Pt electrodes with the quality fraction of the paste.

an acceleration of the  $I_3^-$  reduction. When the concentration of  $H_2PtCl_6$  exceeded 0.6 wt%, the decreased extent of  $R_{ct}$  becomes small.

It is interesting to find that  $R_{ct}$  of the Pt CE drying at  $100^\circ C$  for 4 h, was 3 times larger than that of the Pt CE with hydrothermal treatment for the Pt/ITO-PEN electrode using the same paste (0.6 wt%  $H_2PtCl_6 \cdot 6H_2O$  terpienol solution). This positive effect of hydrothermal treatment is accordant with the surface morphology images as mentioned above. In addition,  $R_{ct}$  of the prepared Pt CEs was comparable to that of the conventional thermal decomposed Pt CEs and much lower than that of the electrodeposited Pt CEs [9].

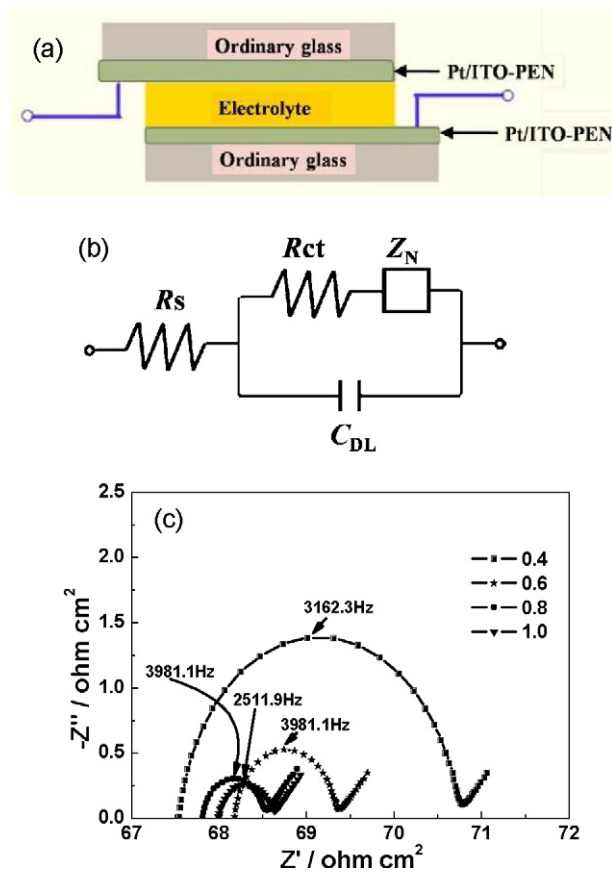


Fig. 4. Schematic structure of cell fabricated by two identical platinized electrodes used in EIS measurements (a), equivalent circuit for EIS (b) and the measured Nyquist plots (c) of the symmetric cells based on Pt CEs prepared by  $H_2PtCl_6 \cdot 6H_2O$  terpienol solution with different concentrations as 0.4 wt% (square), 0.6 wt% (star), 0.8 wt% (circle) and 1.0 wt% (down triangle) followed by hydrothermal treatment.

**Table 1**

The character and performance of Pt electrodes used in DSSCs.

Preparation method	Concentration of $\text{H}_2\text{PtCl}_6 \cdot 6\text{H}_2\text{O}$ (wt%)	Pt-loading ( $\mu\text{g}/\text{cm}^2$ )	$R_{\text{ct}}$ ( $\Omega \text{cm}^2$ )	$J_{\text{sc}}$ ( $\text{mA cm}^{-2}$ )	$V_{\text{oc}}$ (mV)	Conversion efficiency (%)	FF
RH	0.4	2.4	1.38	9.90	676	4.91	0.73
RH	0.6	3.5	0.53	10.1	682	5.41	0.78
RH	0.8	5.8	0.30	9.85	673	4.88	0.74
RH	1.0	7.7	0.26	6.56	673	3.27	0.74
RD	0.6	3.4	1.68	9.30	682	4.05	0.64
TD	0.6	3.7	0.46	11.8	680	5.62	0.70

RH,  $\text{NaBH}_4$  reduction with hydrothermal treatment; RD,  $\text{NaBH}_4$  reduction with directly drying at  $100^\circ\text{C}$  for 4 h; TD, thermal decomposition on ITO-glass.

As a result, the CEs prepared by the paste with higher concentration of  $\text{H}_2\text{PtCl}_6$  usually have lower  $R_{\text{ct}}$  and lower light transmittance. Low  $R_{\text{ct}}$  is beneficial to high performance of CEs, however, low light transmittance of the CEs will decrease the performance of DSSCs in the back illumination model. Therefore, it is necessary to balance between  $R_{\text{ct}}$  and light transmittance. In other words, there is an optimal concentration of  $\text{H}_2\text{PtCl}_6$  for high performance Pt CEs.

The stability of Pt CEs was examined by characterization of electrocatalytic activity in terms of monitoring the  $R_{\text{ct}}$  with time.  $R_{\text{ct}}$  value was increased by 15% compared with the initial value after 12 weeks, which indicates a good stability on the electrocatalytic activity of Pt CEs for triiodide reduction.

### 3.6. Photocurrent–voltage characteristics of flexible DSSCs

Fig. 5 shows configuration of a typical flexible DSSC and the illumination direction through the CE side. The flexible Pt/ITO-PEN CE was leveled up on a piece of ordinary glass. Fig. 6 shows the measured photocurrent–voltage curves of as-fabricated DSSCs and the corresponding photovoltaic parameters are listed in Table 1. The inset of Fig. 6 shows the conversion efficiency of flexible DSSCs as a function of the  $\text{H}_2\text{PtCl}_6$  quality fraction concentration to prepare Pt CEs. The conversion efficiency increases with the  $\text{H}_2\text{PtCl}_6$  concentration and reaches a maximum value at 0.6 wt% then decreases with the concentration. Based on these photovoltaic parameters, the conversion efficiency enhancement is attributable to the promotion of short-circuit current density ( $J_{\text{sc}}$ ) and fill factor (FF) by comparing with the data of the Pt CE without hydrothermal treatment, because their open-circuit voltage ( $V_{\text{oc}}$ ) values were almost unchangeable. It was found that DSSC based on the prepared CE

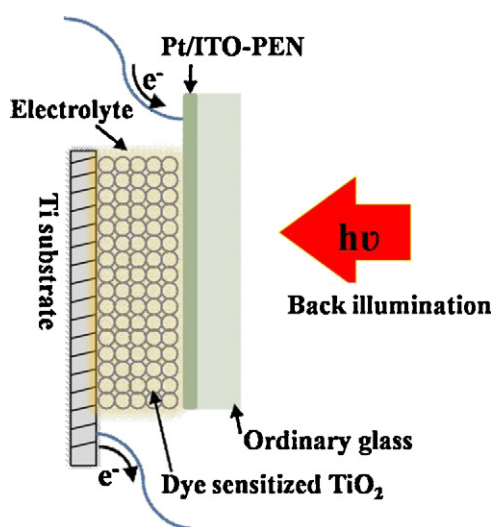


Fig. 5. Configuration of a dye-sensitized solar cell irradiated through the flexible Pt CE (back illumination).

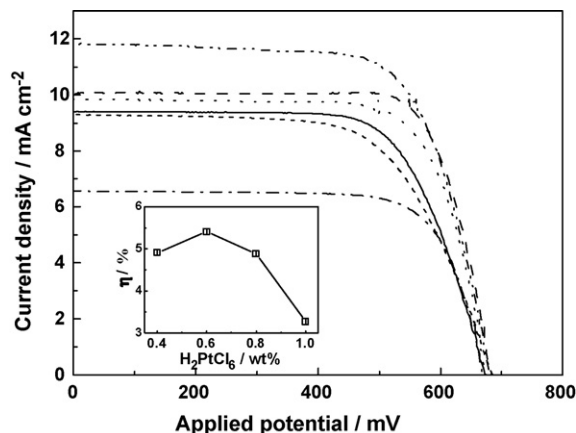


Fig. 6. Current–voltage curves of dye-sensitized solar cells based on Pt CEs prepared with  $\text{H}_2\text{PtCl}_6 \cdot 6\text{H}_2\text{O}$  terphenol solutions with different concentrations as 0.4 wt% (solid line), 0.6 wt% (dash line), 0.8 wt% (dot line) and 1.0 wt% (dash dot line) followed by hydrothermal treatment and with 0.6 wt%  $\text{H}_2\text{PtCl}_6 \cdot 6\text{H}_2\text{O}$  terphenol solution followed by drying at  $100^\circ\text{C}$  for 4 h (short dash line), and thermal deposited Pt electrode on ITO-glass (dash dot dot line). The inset shows the relationships of conversion efficiency of flexible DSSCs with the  $\text{H}_2\text{PtCl}_6$  quality fraction concentration.

without the hydrothermal treatment shows lower fill factor and conversion efficiency. This is consistent with the charge transfer kinetic performance as mentioned above. It is known that FF depends strongly upon the internal resistance of the cell. A higher FF can be obtained for the cell based on Pt CE with the lower resistance of charge transfer on the electrolyte/Pt interface.

However,  $J_{\text{sc}}$  started to decrease when the  $\text{H}_2\text{PtCl}_6$  concentration exceeded 0.6 wt%. The light transmittance of Pt CEs is an important factor for the back-side illumination of the flexible DSSCs. The Pt CE prepared with higher concentration of  $\text{H}_2\text{PtCl}_6$  solution has higher Pt-loading and darker electrode surface, which reduces light intensity illuminated on the photoelectrode, thus giving a lower  $J_{\text{sc}}$  of DSSC. Therefore, to obtain the best performance of DSSCs, there is an optimized point balancing the opposite effect of Pt-loading on  $R_{\text{ct}}$  and the light transmittance. The highest conversion efficiency for DSSC based on Pt CE with Pt-loading of  $3.5 \mu\text{g}/\text{cm}^2$  prepared by 0.6 wt%  $\text{H}_2\text{PtCl}_6$  solution attains 5.41%, which is close to that of DSSC based on the thermal decomposed Pt film (5.62%).

## 4. Conclusions

A flexible DSSC was assembled with a Pt/ITO-PEN CE and a  $\text{TiO}_2$  photoelectrode on Ti foil substrate. The Pt CE was prepared on ITO-PEN using screen printing technology followed by  $\text{NaBH}_4$  reduction combining with hydrothermal method. This chemical reduction method is simple and cheap. The photovoltaic performance of the prepared Pt CEs depends on the  $\text{H}_2\text{PtCl}_6$  concentration, which controls the Pt-loading, thus affects  $R_{\text{ct}}$  and light transmittance of the Pt CEs. The prepared Pt CE shows high electrocatalytic activity for triiodide reduction, and the flexible DSSC fabricated by the Pt CE

prepared with the paste containing 0.6 wt%  $\text{H}_2\text{PtCl}_6 \cdot 6\text{H}_2\text{O}$  terpineol solution and N3 sensitized nanocrystalline- $\text{TiO}_2$  thin film electrode screen printed on Ti foil gives the highest light-to-electricity conversion efficiency of 5.41% at AM 1.5 simulated full sunlight. The satisfied photovoltaic performance of the prepared Pt CEs is attributed to the hydrothermal treatment, in which process the organic residues is removed, and thus decreasing  $R_{\text{ct}}$  of the prepared Pt CEs.

### Acknowledgements

This work was supported by the National Nature Science Foundation of China (no. 20975012), the 111 Project (B07012), the Major State Basic Research Development Program (2006CB202605), the High-Tech Research and Development Program of China (no. 2007AA05Z439).

### References

- [1] B. O'Regan, M. Grätzel, *Nature* 353 (1991) 737.
- [2] M. Grätzel, *J. Photochem. Photobiol. C* 4 (2003) 145.
- [3] M. Grätzel, *J. Photochem. Photobiol. A* 164 (2004) 3.
- [4] N. Takurou, A. Murakami, M. Grätzel, *Inorg. Chim. Acta* 361 (2008) 572.
- [5] M. Grätzel, *J. Photochem. Photobiol. A: Chem.* 164 (2004) 3.
- [6] M.K. Nazeeruddin, F.D. Angelis, S. Fantacci, A. Selloni, G. Viscardi, P. Liska, S. Ito, B. Takeru, M. Grätzel, *J. Am. Chem. Soc.* 127 (2005) 16837.
- [7] Y. Chiba, A. Islam, Y. Watanabe, R. Komiya, N. Koide, L. Han, *Jpn. J. Appl. Phys.* 45 (2006) L638.
- [8] T.C. Wei, C.C. Wan, Y.Y. Wang, *Appl. Phys. Lett.* 88 (2006) 103122.
- [9] S.S. Kim, Y.C. Nah, Y.Y. Noh, J. Jo, D.Y. Kim, *Electrochim. Acta* 51 (2006) 3814.
- [10] M. Ikegami, K. Miyoshi, T. Miyasak, *Appl. Phys. Lett.* 90 (2007) 153122.
- [11] F.S. Cai, J. Liang, Z.L. Tao, J. Chen, R.S. Xu, S.S. Kim, Y.C. Nah, Y.Y. Noh, J. Jo, D.Y. Kim, *J. Power Sources* 177 (2008) 631.
- [12] K. Imoto, K. Takatashi, T. Yamaguchi, T. Komura, J. Nakamura, K. Murata, *Sol. Energy Mater. Sol. Cells* 79 (2003) 459.
- [13] T. Kuboa, J. Tanimoto, M. Minami, T. Toya, Y. Nishikitani, H. Watanabe, *Solid State Ionics* 165 (2003) 97.
- [14] K. Suzuki, M. Yamamoto, M. Kumagai, S. Yanagida, *Chem. Lett.* 32 (2003) 28.
- [15] Z. Huang, X.Z. Liu, K.X. Li, D.M. Li, Y.H. Luo, H. Li, W.B. Song, L.Q. Chen, Q.B. Meng, *Electrochem. Commun.* 9 (2007) 596.
- [16] W.J. Lee, E. Ramasamy, D.Y. Lee, J.S. Song, *Sol. Energy Mater. Sol. Cells* 92 (2008) 814.
- [17] K.X. Li, Y.H. Luo, Z.X. Yu, M.H. Deng, D.M. Li, Q.B. Meng, *Electrochem. Commun.* 11 (2009) 1346.
- [18] Y. Saito, T. Kitamura, Y. Wada, S. Yanagida, *Chem. Lett.* 31 (2002) 1060.
- [19] Y. Saito, W. Kubo, T. Kitamura, Y. Wada, S. Yanagida, *J. Photochem. Photobiol. A: Chem.* 164 (2004) 153.
- [20] J.G. Chen, H.Y. Wei, K.C. Ho, *Sol. Energy Mater. Sol. Cells* 91 (2007) 1472.
- [21] W.J. Hong, Y.X. Xu, G.W. Lu, C. Li, G.Q. Shi, *Electrochem. Commun.* 10 (2008) 1555.
- [22] P. Balraju, M. Kumar, M.S. Roy, G.D. Sharma, *Synth. Met.* 159 (2009) 1325.
- [23] K.M. Lee, P.Y. Chen, C.Y. Hsu, J.H. Huang, W.H. Ho, H.C. Chen, K.C. Ho, *J. Power Sources* 188 (2009) 313.
- [24] J.H. Wu, Q.H. Li, L.Q. Fan, Z. Lan, P.J. Li, J.M. Lin, S.C. Hao, *J. Power Sources* 181 (2008) 172.
- [25] Q.H. Li, J.H. Wu, Q.W. Tang, Z. Lan, P.J. Li, J.M. Lin, L.Q. Fan, *Electrochem. Commun.* 10 (2008) 1299.
- [26] X.M. Fang, T.L. Ma, M. Akiyama, G.Q. Guan, S. Tsunematsu, E. Abe, *Thin Solid Films* 472 (2005) 242.
- [27] M. Grätzel, *Chem. Commun.* 38 (2006) 4004.
- [28] M.G. Kang, N.G. Park, K.S. Ryu, S.H. Chang, K.J. Kim, *Sol. Energy Mater. Sol. Cells* 90 (2006) 574.
- [29] J.H. Park, Y. Jun, H.G. Yun, S.Y. Lee, M.G. Kang, *J. Electrochem. Soc.* 155 (2008) F145.
- [30] G.Q. Wang, R.F. Lin, Y. Lin, X.P. Li, X.W. Zhou, X.R. Xiao, *Electrochim. Acta* 50 (2005) 5546.
- [31] X. Yin, W.W. Tan, J.B. Zhang, Y.X. Weng, X.R. Xiao, X.W. Zhou, X.Q. Li, Y. Lin, *Colloids Surf. A* 326 (2008) 42.
- [32] J.M. Chen, Y.P. Zou, Y.F. Li, X.W. Zhou, J.B. Zhang, X.P. Li, X.R. Xiao, Y. Lin, *Chem. Phys. Lett.* 460 (2008) 168.
- [33] G.Q. Wang, Y. Lin, X.R. Xiao, X.P. Li, W.B. Wang, *Surf. Interface Anal.* 36 (2004) 1437.
- [34] N. Papageorgiou, W.F. Maier, M. Grätzel, *J. Electrochem. Soc.* 144 (1997) 876.